

# Entropy Generation Analyses for Couette-Poiseuille Slip Flow in a Micro-annulus

Sanaz Mirzaparikhany<sup>\*1</sup>, Mehran Abdoulalipouradi<sup>\*2</sup>, Mortaza Yari<sup>\*3</sup>

<sup>1</sup>Department of Mechanical Engineering, University of Mohaghegh Ardabili, Ardabil, Iran

<sup>2</sup>Department of Mechanical Engineering, University of Tabriz, Tabriz, Iran

<sup>3</sup>Faculty of Engineering, University of Mohaghegh Ardabili, Ardabil, Iran

<sup>1</sup>s.parikhany@gmail.com; <sup>2</sup>mehran\_abdoulalipouradi@yahoo.com; <sup>3</sup>myari@uma.ac.ir

**Abstract-** In this study, entropy generation of fluid flow in axially moving micro-concentric cylinders for the Couette-Poiseuille slip flow was studied. Fully developed laminar flow was considered with uniform heat flux at the walls. The effects of slip velocity, temperature jump at the walls, and viscous dissipation were taken into consideration. The velocity and temperature profiles were obtained analytically and used to compute the entropy generation. The obtained results were compared with the available data in the literature and an excellent agreement was observed. Effects of Knudsen number, cylinder moving velocity, cylinders radius ratio, Brinkman number and  $Br/\Omega$  on the entropy generation were also investigated. It was found that by increasing the Knudsen number and cylinder moving velocity the entropy generation is decreased, while any increase in cylinders radius ratio, Brinkman number, and also  $Br/\Omega$  causes the entropy generation to be increased. It was also found that the fluid friction is the main reason for the entropy generation for flow in the annulus region.

**Keywords-** Entropy Generation Minimization; Second Laws of Thermodynamics Analysis; Viscous Dissipation; Slip Flow and Temperature Jump; Couette-Poiseuille Flow

## I. INTRODUCTION

Fluid flow in micro channels has emerged as an important area of research. This has been motivated by their various applications such as medical and biomedical use, computer chips, and chemical separations. The advent of micro-electro-mechanical systems (MEMS) has opened up a new research area where non-continuum behaviour is important. MEMS are one of the major advances of industrial technologies in the past decades. Micron size mechanical and biochemical devices are becoming more prevalent both in commercial applications and in scientific research. The extensive engineering applications of microchannels have promoted abundant studies on their fluid flow and heat transfer characteristics. Besides the analysis based on the basic conservation laws, the second-law analysis is crucial in understanding the entropy generation attributed to the thermodynamic irreversibility, which is useful for studying the optimum operating conditions in designing a system with less entropy generation [1].

Recently, Marques et al. analyzed the Couette flow with slip and jump boundary conditions for parallel plates. They analyzed the steady plane Couette flow within the framework of the five field equations of mass, momentum and energy for a Newtonian viscous heat conducting ideal gas by considering the slip and jump boundary conditions [2]. Haddad et al. investigated numerically the entropy generation due to steady laminar forced convection fluid flow through parallel plate microchannel. The effects of Knudsen, Reynolds, Prandtl, and Eckert numbers and also the nondimensional temperature difference on entropy generation within the microchannel were investigated [3]. Aydin and Avci studied laminar forced convective heat transfer for a Newtonian fluid in a micropipe by taking the viscous dissipation effect, the velocity slip, and the temperature jump at the wall into account. They examined the hydrodynamically and thermally fully developed flow case by considering two different thermal boundary conditions i.e., the constant heat flux (CHF) and the constant wall temperature (CWT) [4-6]. Hooman presented the closed form solutions for fully developed temperature distribution and entropy generation due to forced convection in MEMS in the slip-flow regime, for which the Knudsen number lies within the range  $0.001 < Kn < 0.1$ . Two different cross-sections were analyzed, being microducts and micropipes, by including the effects of viscous dissipation [7]. Barkhordari and Etemad performed numerical simulations to study flow and thermal fields of non-Newtonian fluids in circular microchannels. The flow was considered to be slip, axisymmetric, steady, incompressible, and laminar and the power law model was used to characterize the behavior of the non-Newtonian fluid. The constant wall heat flux and constant wall temperature were employed as thermal boundary conditions [8]. Sun et al. investigated the steady-state convective heat transfer for laminar, two-dimensional, and incompressible rarefied gas flow in the thermal entrance region of a tube under constant wall temperature, constant wall heat flux, and linear variation of wall temperature boundary conditions. The study was performed by finite-volume finite difference scheme with slip flow and temperature jump conditions [9]. Avci and Aydin applied the second-law analysis of thermodynamics to two different micro geometries including microtube and microducts, between two parallel plates. They carried out a parametric study on hydrodynamically and thermally fully developed slip-flow with constant properties to determine the combined effects of the Brinkman and Knudsen numbers on the entropy generation [10]. Avci and Aydin also studied an analytical solution to forced convective heat transfer in hydrodynamically and thermally fully developed slip-flows of viscous dissipation gases in annular microducts between two concentric micro cylinders. Two different cases of the thermal boundary conditions were considered including the uniform heat flux at the outer wall and

adiabatic inner wall and the uniform heat flux at the inner wall and adiabatic outer wall [11]. Hooman presented superposition approach to investigate forced convection in microducts of arbitrary cross-section, subjected to the H1 (constant wall temperature) and H2 (uniform heat flux at the walls) boundary conditions, in the slip-flow regime with further complication of a temperature jump condition assumption. It was shown that applying an average slip velocity and temperature jump definition, one can use the no-slip/no-jump results with some minor modifications [12]. Yari presented the first and second laws of thermodynamics analysis for laminar forced convective heat transfer for a Newtonian fluid in a microchannel between parallel plates for Couette-Poiseuille flow. Hydrodynamically and thermally fully developed flow with constant properties was examined. Entropy generation was shown to decrease with an increase in Kn while increasing Br and Br/Ω results in increasing the entropy generation [13].

For flow inside a micro annulus, Yari investigated the entropy generation in a micro-annulus flow. Fully developed laminar flow was considered with uniform heat flux at the walls. The viscous dissipation effect, the velocity slip, and the temperature jump at the wall were taken into consideration. The velocity and temperature profiles were obtained analytically and used to compute the entropy generation rate. Entropy generation was shown to decrease with an increase in Kn while increasing Br, Br/Ω and r\* resulted in increasing the entropy generation [14]. Khadrawi and Al-Shyyab studied the hydrodynamics and thermal behaviors of fluid flow in axially moving micro-concentric cylinders. The viscous dissipation, slip flow, and temperature jump at the walls were considered. They also assumed no significant gradient of pressure in the x and r directions. The velocity and temperature profiles obtained analytically and data optioned using a symbolic algebraic equation solver code. It was shown that as Kn increases the slip in the hydrodynamic and thermal boundary condition is also increased. The slip and jump at the inner surface were much larger than that of the outer one and the slip velocity vanishes when the outer cylinder velocity approaches the inner cylinder one [15].

According to our knowledge, there is a lack of information in the literature regarding the second-law analysis and entropy generation for heat transfer and fluid flow through axially moving cylinder by taking into account the effects of viscous dissipation, slip velocity, and temperature jump. Thus, the aim of this paper is to analyse analytically the entropy generation of Couette-Poiseuille slip flow in a micro-annulus.

## II. MATHEMATICAL MODEL

Consider two long concentric cylinders with a viscous fluid between them, as shown in Fig. 1. The Outer cylinder moves axially with relative velocity V, than the inner cylinder. In the analysis, the flow is considered to be fully developed both hydrodynamically and thermally. Steady, laminar flow having constant properties is considered. The axial heat conduction in the fluid and the wall is assumed to be negligible.

### A. Hydrodynamic Aspects

The equation of motion for flow with aforementioned assumptions for a cylindrical geometry in the x-direction is described as:

$$\frac{1}{r} \frac{\partial}{\partial r} \left( r \frac{\partial u}{\partial r} \right) = \frac{1}{\mu} \frac{dP}{dx} \quad (1)$$

That P is the pressure of flow and  $\frac{dP}{dx}$  is the pressure gradient in flow.

Hydrodynamic boundary conditions are:

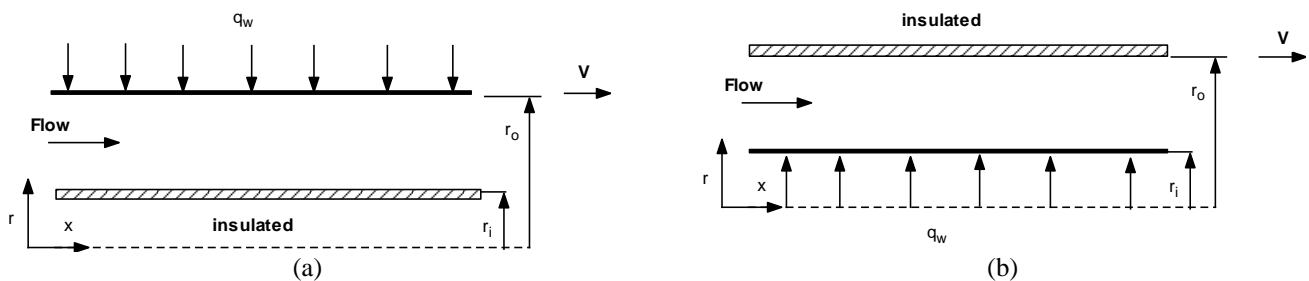


Fig. 1 Geometry and schematic diagram of flow domain: (a) Case A; (b) Case B

$$r = r_i, \quad u = u_i \quad (2)$$

$$r = r_o, \quad u = V - u_s \quad (3)$$

where,  $u_s$  is the slip velocity which for a cylindrical geometry can be expressed as [4]:

$$u_s = -\frac{2-F}{F} \lambda \left. \frac{\partial u}{\partial r} \right|_{wall} \quad (4)$$

where,  $\lambda$  is the mean free path,  $F$  is the momentum accommodation factor which is close to unity for most of the gas solid couples used in engineering applications and taken so herein. By using the following dimensionless parameters:

$$R = \frac{r}{r_o}, \quad r^* = \frac{r_i}{r_o}, \quad \bar{u} = \frac{u}{u_m}, \quad \bar{v} = \frac{V}{u_m} \quad (5)$$

The fully developed velocity profile can be determined by solving Eq. (1) together with the slip boundary conditions given in Eqs. (2) and (3) as:

$$\bar{u} = (1-\bar{v}) \frac{1-R^2 + 2r_m^{*2} \ln R + a}{\frac{b}{2}} + \bar{v} \quad (6)$$

where,  $a$  and  $b$  are:

$$a = 2Kn(1-r^*)(1-r_m^{*2}) \quad (7)$$

$$b = 1-r^{*2} - 4r_m^{*2} \left( \frac{1}{2} + \frac{r^{*2}}{1-r^{*2}} \ln r^* \right) + 2a \quad (8)$$

where,  $Kn$  is Knudsen number ( $Kn = \frac{\lambda}{2(r_o - r_i)}$ ) and  $r_m^*$  designates the dimensionless radius where the maximum velocity occurs and is given by:

$$r_m^{*2} = \frac{(1-r^{*2})(1+4Kn) + b \frac{\bar{v}}{u-v}}{2 \ln\left(\frac{1}{r^*}\right) - 4Kn\left(\frac{r^{*2}-1}{r^*}\right)} \quad (9)$$

### B. First-law analysis

The steady-state energy equation for laminar flow under the assumption conditions can be written as:

$$u \frac{\partial T}{\partial x} = \frac{\alpha}{r} \frac{\partial}{\partial r} \left( r \frac{\partial T}{\partial r} \right) + \frac{\mu}{\rho C_p} \left( \frac{\partial u}{\partial r} \right)^2 \quad (10)$$

The thermal boundary conditions for case A and B are:

$$\text{Case A : } \begin{cases} r = r_i \\ \frac{\partial T}{\partial r} = 0 \end{cases}, \quad \begin{cases} r = r_o \\ T = T_s \end{cases} \quad (11)$$

$$\text{Case B : } \begin{cases} r = r_i \\ T = T_s \end{cases}, \quad \begin{cases} r = r_o \\ \frac{\partial T}{\partial r} = 0 \end{cases} \quad (12)$$

where,  $T_s$  is the temperature jump which for cylindrical geometry can be expressed as [4]:

$$T_s - T_w = -\frac{2-F_t}{F_t} \frac{2\gamma}{1+\gamma} \frac{\lambda}{Pr} \left. \frac{\partial T}{\partial r} \right|_{wall} \quad (13)$$

where,  $\gamma$  is the specific heat ratio,  $Pr$  is the prandtl number of the fluid and  $F_t$  is the thermal accommodation factor, which depends on the gas and surface metal such is assumed typical value near unity for air.

For the uniform wall heat flux case and thermally fully developed flow, the first term in the left side of Eq. (10) is [16]:

$$\frac{\partial T}{\partial x} = \frac{\partial T_w}{\partial x} = \frac{\partial T_m}{\partial x} \quad (14)$$

With isoflux walls, following the application of the first-law of thermodynamics, the longitudinal bulk temperature gradient in the fully developed is as follows [7]:

$$m \cdot C_p \frac{\partial T_m}{\partial x} = q_w p + \int \mu \left( \frac{du}{dr} \right)^2 dA \quad (15)$$

Where,  $p$  is the heated perimeter of the micro channel. By introduction the following non dimensional temperature:

$$\theta = \frac{T - T_s}{q_w r_o / k} \quad (16)$$

Eq. (10) can be written as:

$$\text{Case A: } \frac{1}{R} \frac{d}{dR} \left( R \frac{d\theta}{dR} \right) = \frac{2a_0}{1-r^{*2}} \bar{u} - Br \left( \frac{\partial \bar{u}}{\partial R} \right)^2 \quad (17)$$

$$\text{Case B: } \frac{1}{R} \frac{d}{dR} \left( R \frac{d\theta}{dR} \right) = \frac{2a_0 r^*}{1-r^{*2}} \bar{u} - Br \left( \frac{\partial \bar{u}}{\partial R} \right)^2 \quad (18)$$

where,  $Br$  is the Brinkman Number ( $Br = \frac{\mu u_m^2}{q_w r_o}$ ), and  $a_0$  is:

$$\text{Case A: } a_0 = 1 + 16Br \frac{(1-\bar{v})^2}{b^2} \left[ \frac{1-r^{*4}}{4} - r_m^{*4} \ln r^* - r_m^{*2} (1-r^{*2}) \right] \quad (19)$$

$$\text{Case B: } a_0 = 1 + 16Br \frac{(1-\bar{v})^2}{r^* b^2} \left[ \frac{1-r^{*4}}{4} - r_m^{*4} \ln r^* - r_m^{*2} (1-r^{*2}) \right] \quad (20)$$

For case A, solution of Eq. (17) under thermal boundary conditions given in Eq. (11) is obtained as:

$$\theta = \frac{a_0 \bar{v}}{2(1-r^{*2})} R^2 + \frac{4a_0(1-\bar{v})}{b(1-r^{*2})} \left[ \frac{R^2}{4} - \frac{R^4}{16} - \frac{r_m^{*2}}{4} R^2 - r_m^{*2} \frac{R^2}{2} \left( \frac{1}{2} - \ln R \right) + \frac{a}{4} R^2 \right] - 16Br \frac{(1-\bar{v})^2}{b^2} \left[ \frac{r_m^{*2}}{2} (\ln R)^2 + \frac{R^4}{16} - \frac{r_m^{*2} R^2}{2} \right] + c_1 \ln R + c_2 \quad (21)$$

where,  $c_1$  and  $c_2$  can be obtained by applying the boundary conditions:

$$0 = \frac{a_0 \bar{v}}{1-r^{*2}} r^* + \frac{4a_0(1-\bar{v})}{b(1-r^{*2})} \left[ \frac{r^*}{4} - \frac{r^{*3}}{4} - \frac{r_m^{*2}}{2} r^* - r_m^{*2} r^* \ln r^* + \frac{a}{2} r^* \right] - 16Br \frac{(1-\bar{v})^2}{b^2} \left[ \frac{r_m^{*2}}{r^*} \ln r^* + \frac{r^{*3}}{4} - r_m^{*2} r^* \right] + \frac{c_1}{r^*} \quad (22)$$

$$0 = \frac{a_0 \bar{v}}{2(1-r^{*2})} + \frac{4a_0(1-\bar{v})}{b(1-r^{*2})} \left[ \frac{3}{16} - \frac{r_m^{*2}}{2} + \frac{a}{4} \right] - 16Br \frac{(1-\bar{v})^2}{b^2} \left[ \frac{1}{16} - \frac{r_m^{*2}}{2} \right] + c_2 \quad (23)$$

For case B:

$$\theta = \frac{a_0 \bar{v}}{2(1-r^{*2})} r^* R^2 + \frac{4a_0(1-\bar{v})}{b(1-r^{*2})} r^* \left[ \frac{R^2}{4} - \frac{R^4}{16} - \frac{r_m^{*2}}{4} R^2 - r_m^{*2} \frac{R^2}{2} \left( \frac{1}{2} - \ln R \right) + \frac{a}{4} R^2 \right] - 16Br \frac{(1-\bar{v})^2}{b^2} \left[ \frac{r_m^{*2}}{2} (\ln R)^2 + \frac{R^4}{16} - \frac{r_m^{*2} R^2}{2} \right] + c_3 \ln R + c_4 \quad (24)$$

$$0 = \frac{a_0 \bar{v}}{2(1-r^{*2})} r^* + \frac{4a_0(1-\bar{v})}{b(1-r^{*2})} r^* \left[ \frac{1}{2} - \frac{r_m^{*2}}{2} + \frac{a}{2} \right] - 16Br \frac{(1-\bar{v})^2}{b^2} \left[ \frac{1}{4} - r_m^{*2} \right] + c_3 \quad (25)$$

$$0 = \frac{a_0 \bar{v}}{2(1-r^{*2})} r^{*3} + \frac{4a_0(1-\bar{v})}{b(1-r^{*2})} r^* \left[ \frac{r^{*2}}{4} - \frac{r^{*4}}{16} - \frac{3}{4} r_m^{*2} r^{*2} - r_m^{*2} \ln r^* + \frac{a}{4} r^{*2} \right] - 16Br \frac{(1-\bar{v})^2}{b^2} \left[ \frac{r^{*4}}{16} - \frac{r_m^{*2} r^*}{2} \right] + c_3 \ln r^* + c_4 \quad (26)$$

### C. Second-law analysis

According to Bejan [17], the volumetric rate of entropy generation is defined as:

$$\dot{S}_{gen}''' = \frac{k}{T_0^2} \nabla T^2 + \frac{1}{T_0} \phi \quad (27)$$

That  $\phi$  is the dissipation function and for cylindrical coordinates defined as:  $\phi = \mu \left[ \left( \frac{\partial u}{\partial r} \right)^2 + \left( \frac{\partial v}{r \partial \theta} \right)^2 + \left( \frac{\partial u}{r \partial \theta} + \frac{\partial v}{\partial r} \right)^2 \right]$ , with

assumptions of flow it becomes  $\phi = \mu \left( \frac{\partial u}{\partial r} \right)^2$  [16]. Therefore Eq. (27) can be written as:

$$\dot{S}_{gen}''' = \frac{k}{T_0^2} \left( \frac{\partial T}{\partial r} \right)^2 + \frac{\mu}{T_0} \left( \frac{\partial u}{\partial r} \right)^2 \quad (28)$$

where,  $T_0$  is the reference temperature [18]. The dimensionless form of entropy generation rate is entropy generation number ( $N_s$ ) which is equal to the ratio of the actual entropy generation to the characteristics entropy transfer rate [19]. Using the non-dimensional quantities, the eq. (28) can be expressed as:

$$N_s = \frac{\dot{S}_{gen}'''}{S_{G,C}} = \left( \frac{\partial \theta^*}{\partial R} \right)^2 + \frac{Br}{\Omega} \left( \frac{\partial u}{\partial R} \right)^2 = N_H + N_F \quad (29)$$

where,  $\theta^*$  is [4, 7]:

$$\theta^* = \theta - \frac{4\gamma}{1+\gamma} \frac{Kn}{Pr} (1-r^*) \quad (30)$$

and  $\Omega$  is the dimensionless temperature difference:

$$\Omega = \frac{T_w - T_0}{T_0} \quad (31)$$

$S_{G,C}$  in Eq. (29) is the characteristics entropy transfer rate, defined as:

$$S_{G,C} = \frac{q_w^2}{T_0^2 k} \quad (32)$$

The average entropy generation rate (over a cross-section),  $N_{s,ave}$ , can be defined as follows:

$$N_{s,ave} = \frac{\int N_s dA}{A} = 2 \frac{\int N_s R dR}{1-r^{*2}} \quad (33)$$

### D. Analysis validation

In order to validate the present model, the simulation results have been compared with the available numerical data for simplified cases from Yari [14], Avci and Aydin [11] and Kays et. Al. [16] which are given in Fig. 2, Table 1 and Table 2. As seen, an excellent agreement is obtained.

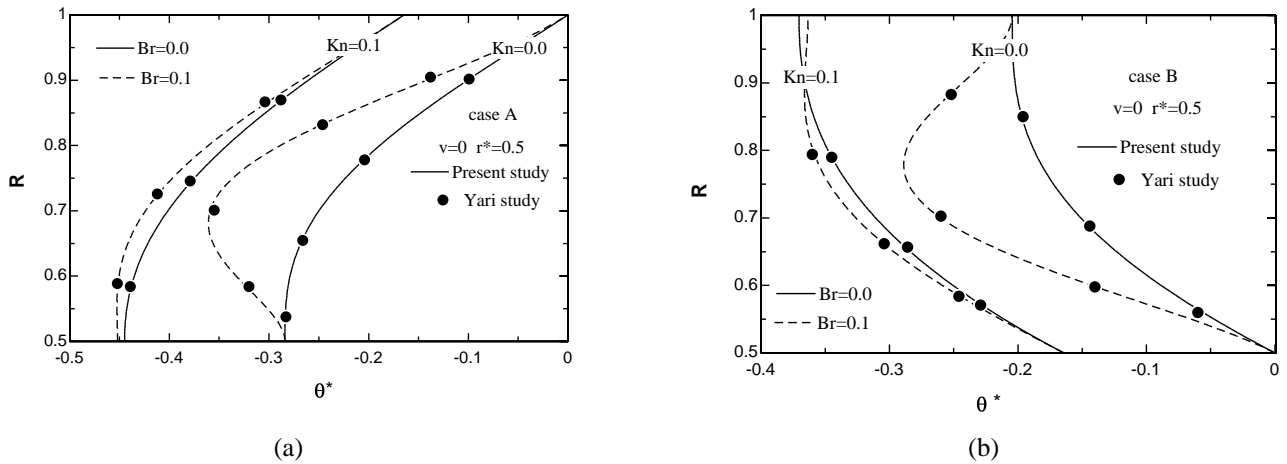


Fig. 2 Comparison of dimensionless temperature distributions for present study and available results from the Yari [14]

TABLE 1 COMPARISON NUSSLETT NUMBERS FOR PRESENT STUDY AND AVAILABLE RESULTS FROM [11, 14] FOR DIFFERENT VALUES  $r^*$  AT  $Kn=0$ ,  $Br=0$  AND  $\bar{v} = 0$

$r^*$	Case A		Case B	
	Present study	Avci and Aydin [11] Yari [14]	Present study	Avci and Aydin [11] Yari [14]
0.2	4.88251	4.88259	8.49933	8.49892
0.4	4.98023	4.97917	6.58393	6.58330
0.6	5.09960	5.09922	5.90542	5.91171
0.8	5.23636	5.23654	5.57707	5.57849

TABLE 2 COMPARISON NUSSLETT NUMBERS FOR PRESENT STUDY AND AVAILABLE RESULTS FROM [16] FOR DIFFERENT VALUES  $r^*$  AT  $Kn=0$ ,  $Br=0$  AND  $\bar{v} = 0$

$r^*$	Case A		Case B	
	Present study	Kays et. al [16]	Present study	Kays et. al [16]
0.2	4.88251	4.883	8.49933	8.499
0.4	4.98023	4.979	6.58393	6.583
0.6	5.09960	5.099	5.90542	5.912
0.8	5.23636	5.24	5.57707	5.58

### III. RESULTS AND DISCUSSION

Fig. 3 exhibits the influence of  $Br/\Omega$  on the entropy generation at  $Kn$  values of 0 and 0.1 and at different values of  $r^*$  and  $\bar{v}$ . This parameter determines the relative importance of the viscous effect. As seen, increasing the value of  $Br/\Omega$  results in increasing the entropy generation due to viscous dissipation. On the other hand, increasing the  $Kn$  value causes the entropy generation to be decreased because of some decrease in the fluid friction. Moreover, entropy generation tends to increase with decreasing  $r^*$ .

The calculations show that the Bejan number is  $Be \rightarrow 0$  ( $N_s \approx N_f$ ), which clearly means that the entropy generation is mainly occurred as a result of the fluid friction. Moreover, the entropy generation is minimized in the region of the annulus where the velocity magnitude is maximum. In addition, entropy generation reaches to a high value in the regions nearby the annulus pipe

walls which is due to the high velocity gradient in these regions. Another point worthy of comment is that the spatial variation of entropy generation is similar to the velocity profile.

Fig. 4 illustrates the variations of  $N_{s,ave}$  against  $R$  at different levels of  $Br/\Omega$  and different values of  $r^*$  and  $\bar{v}$ . It can be seen that the average entropy generation rate is decreased by increasing the  $Kn$  and  $\bar{v}$  values. Furthermore, a direct dependence between the entropy generation and  $\bar{v}$  is observed, so that by increasing the  $\bar{v}$  value, the entropy generation is increased. This is because of increasing in fluid friction by increasing the  $\bar{v}$  value. Fig. 4 also shows that the entropy generation rate could be increased by increasing the value of  $\bar{v}$ . It can be interpreted on this fact that the velocity gradient tends to increase by increasing the  $\bar{v}$  in which case the rate of fluid friction increases in the region of the annulus pipe wall. As observed from Fig. 4, the average entropy generation rate decreases with increasing  $Kn$ , or by increasing  $Br/\Omega$ . Hence, the entropy generation rate due to the fluid friction is increased with an increase in  $Br/\Omega$ . Finally, another feature of considerable interest is that the case A is the most irreversible design while the case B produces the least entropy.

#### IV. CONCLUSION

Entropy generation of fluid flow in axially moving micro-concentric cylinders in the slip flow and temperature jump regime as well as how it varies with  $Kn$ ,  $Br$ ,  $Br/\Omega$ ,  $r^*$  and  $\bar{v}$  were studied. Fully developed laminar flow was considered with uniform heat flux at the walls. The velocity and temperature profiles were obtained analytically and used to compute the entropy generation rate.

The following conclusion can be summarized from this study:

- Entropy generation decreases as  $Kn$  and  $\bar{v}$  increase, while increasing of  $Br$ ,  $Br/\Omega$  and  $r^*$  lead to an increase in the entropy generation.
- Case A is the most irreversible design while case B produces the least entropy generation.

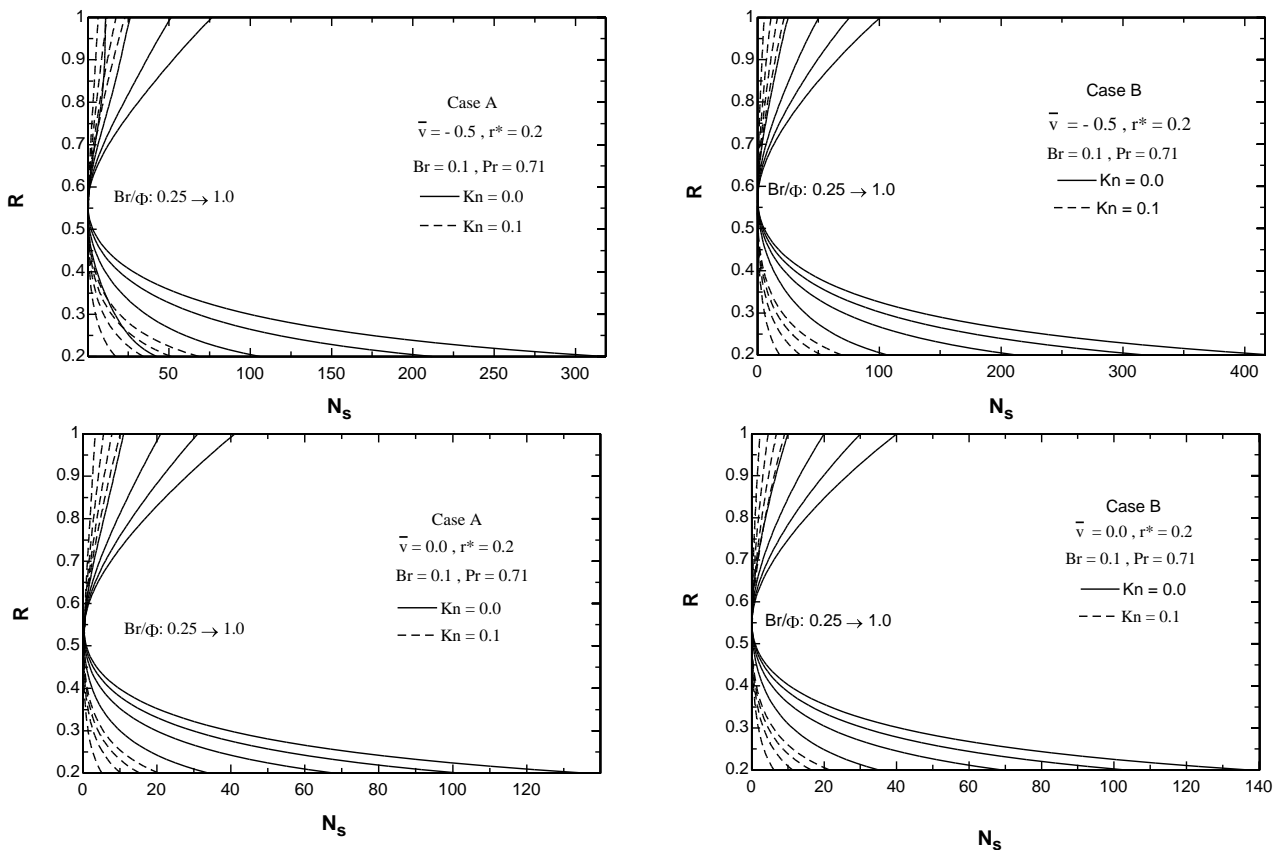
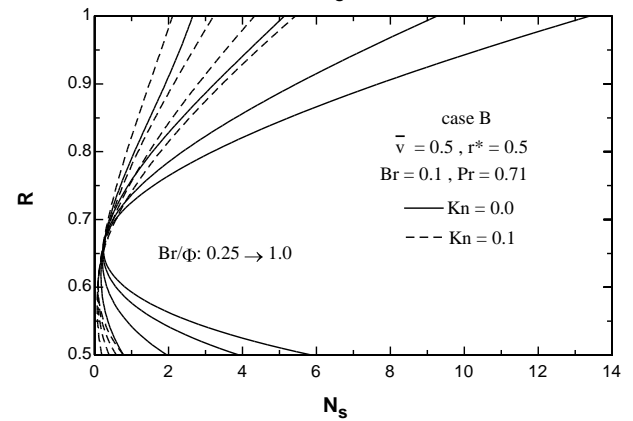
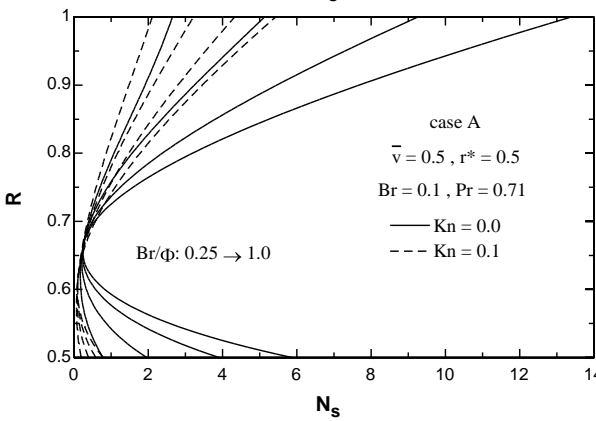
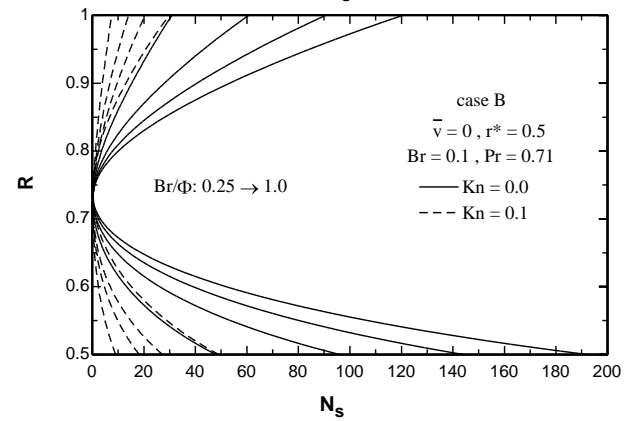
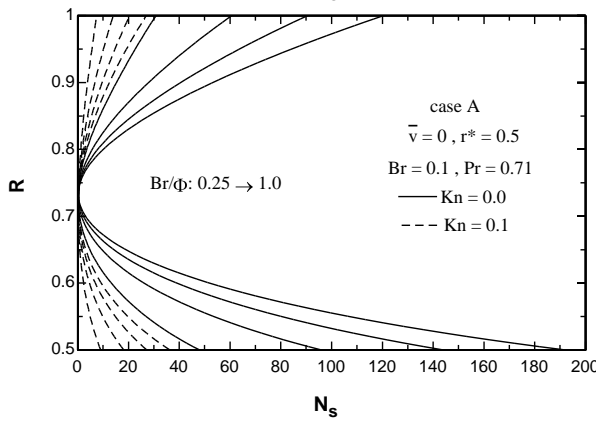
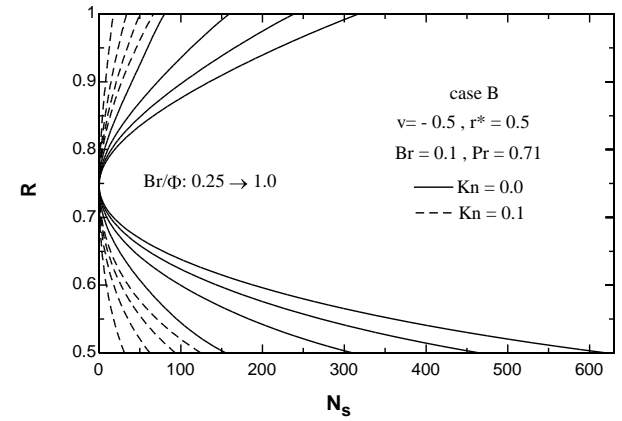
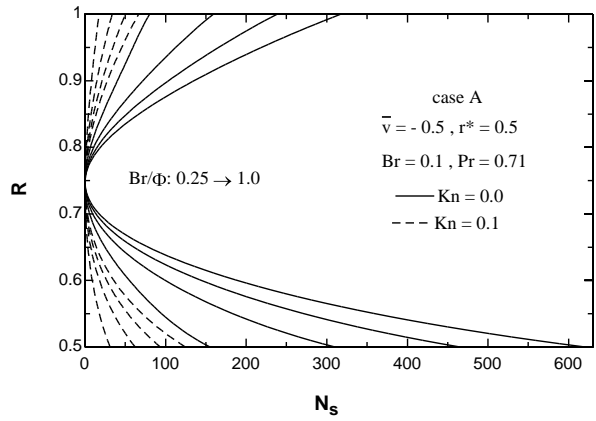
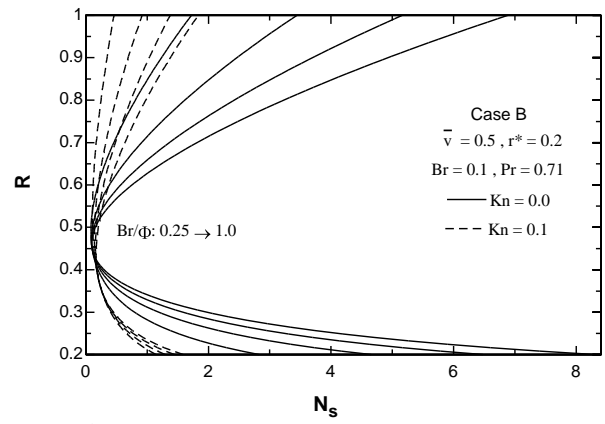
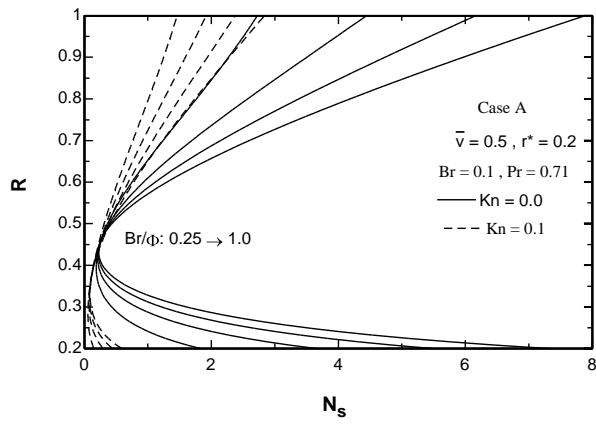


Fig. 3 The variation of  $N_s$  for different values of  $Kn$ ,  $Br/\Omega$  and  $r^*$ : (a) Case A and (b) Case B



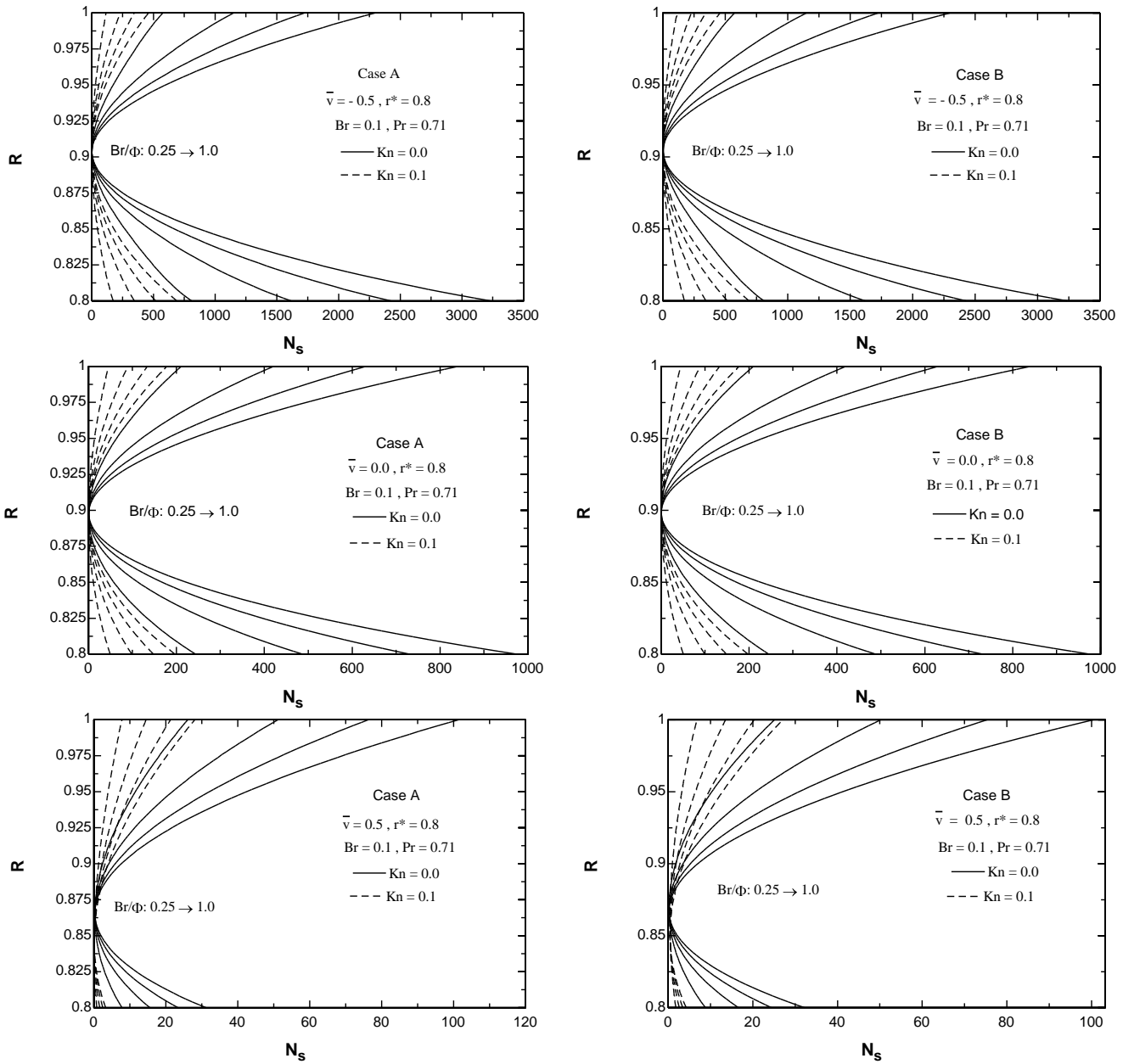
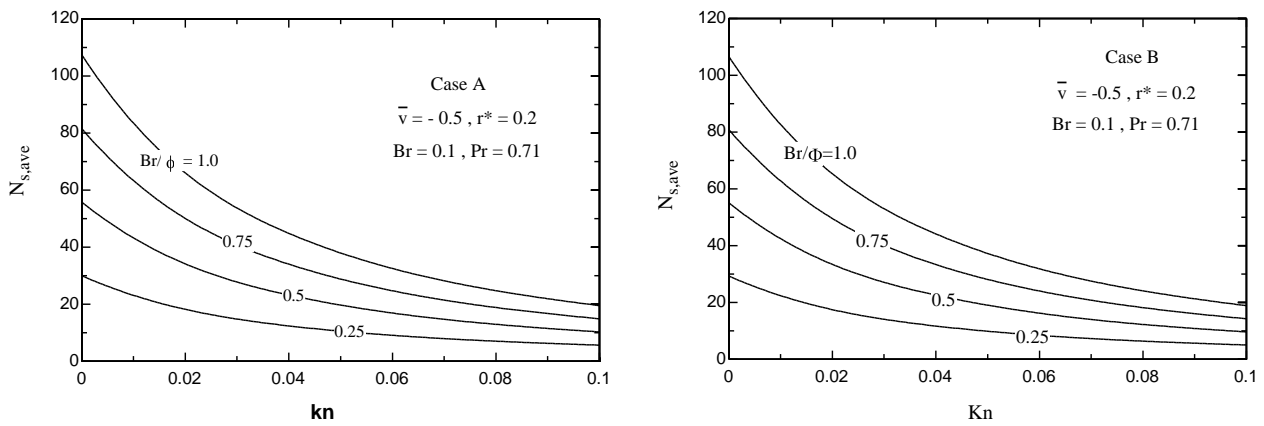


Fig. 3 (Continued)



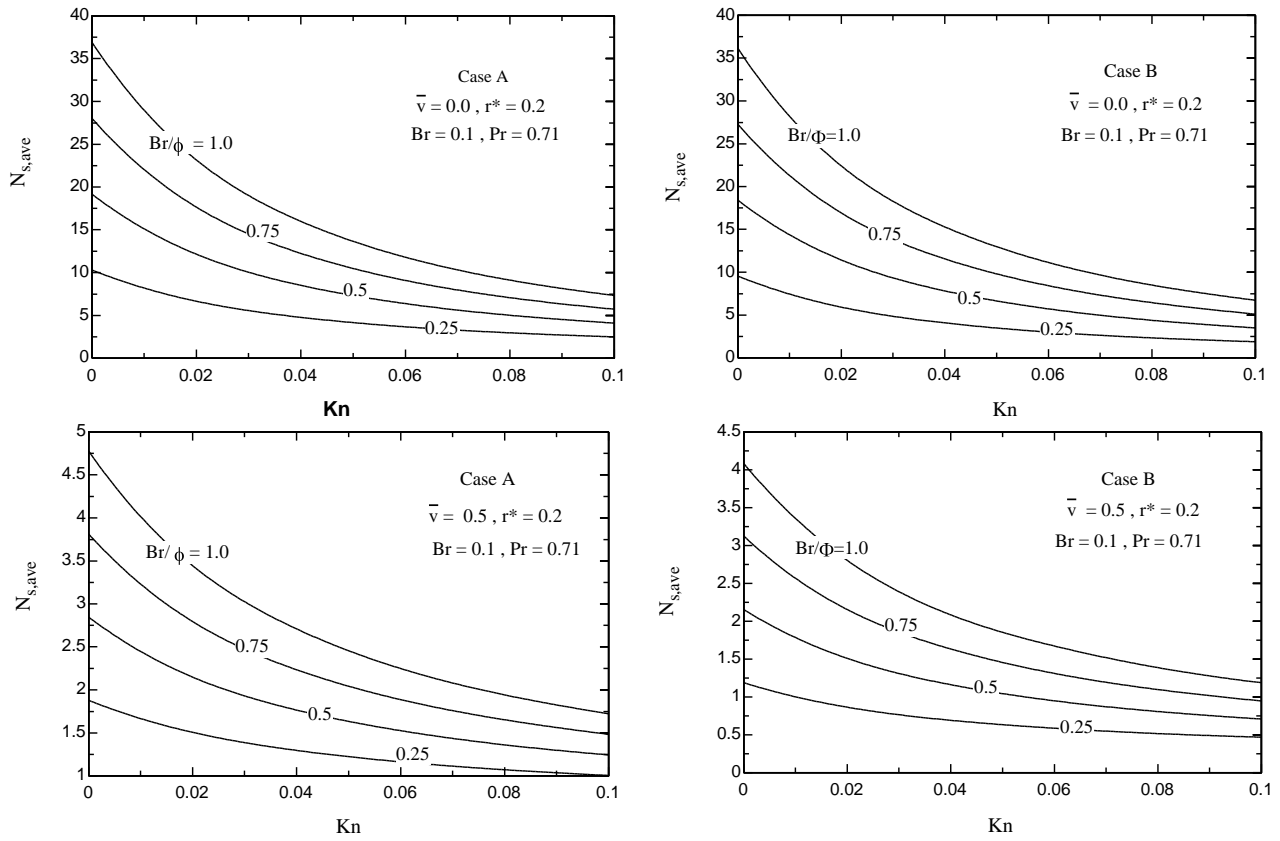
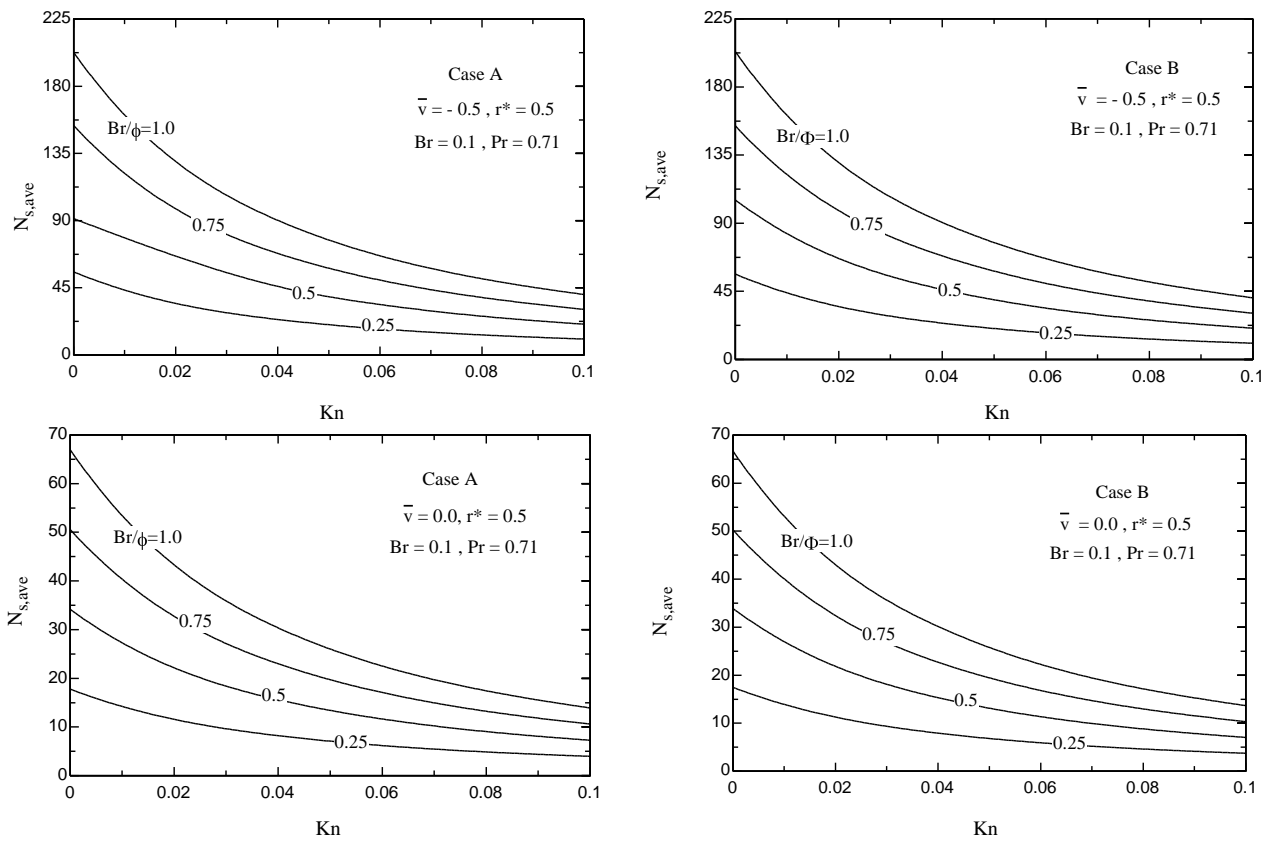
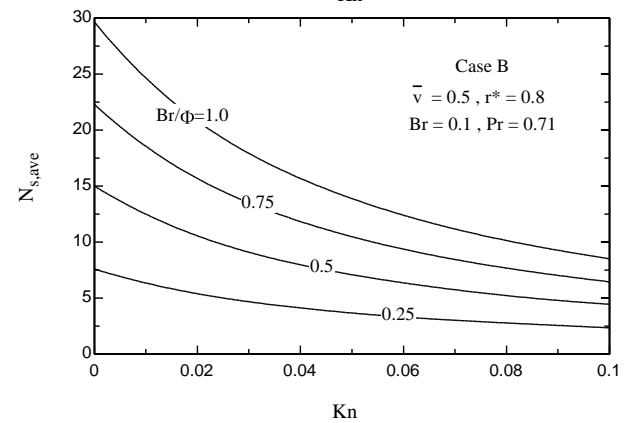
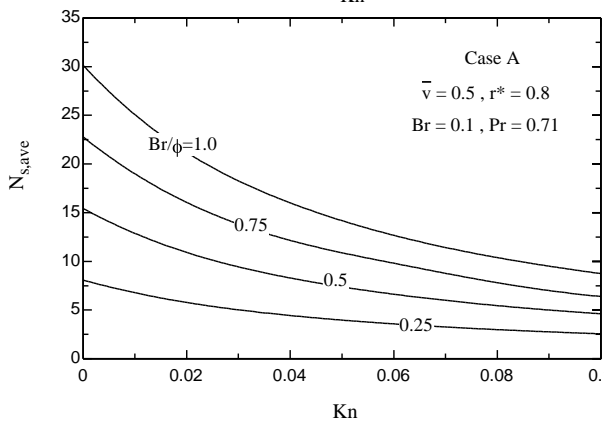
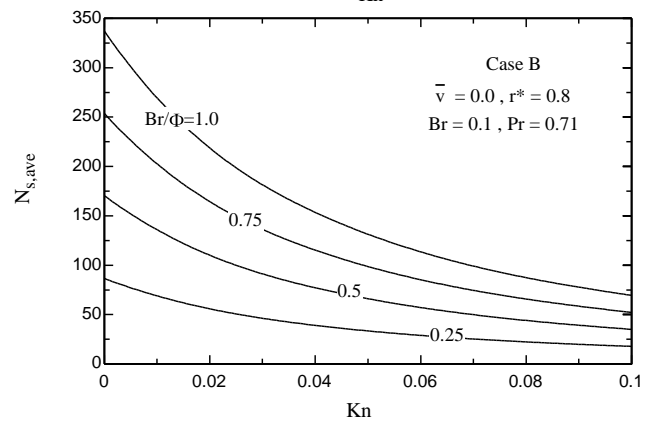
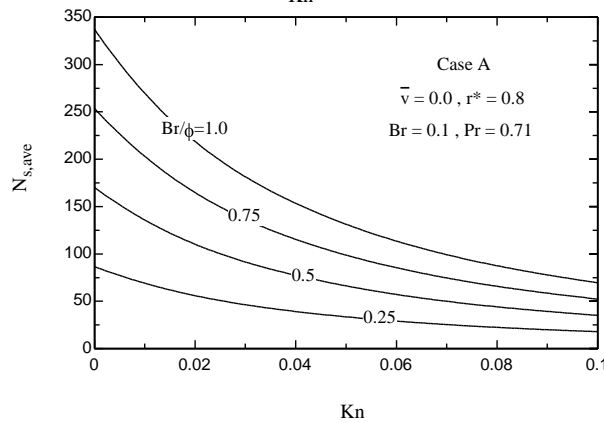
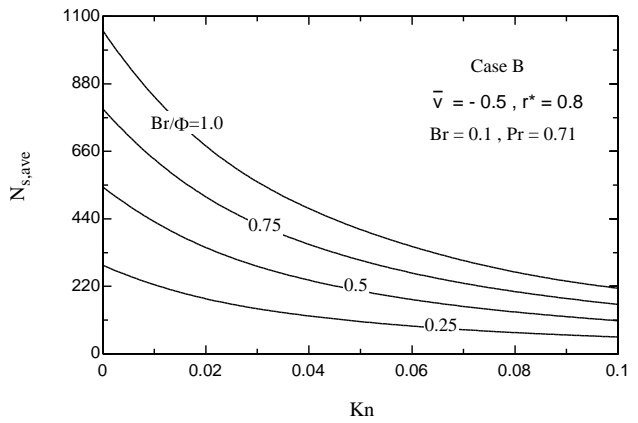
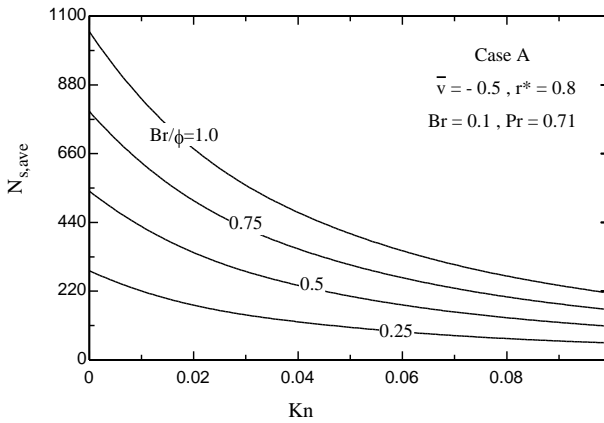
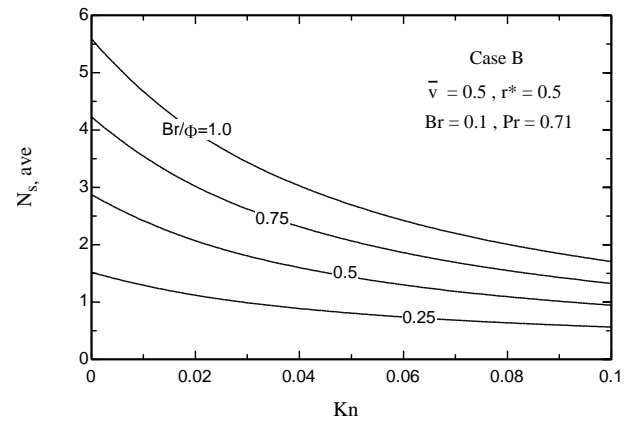
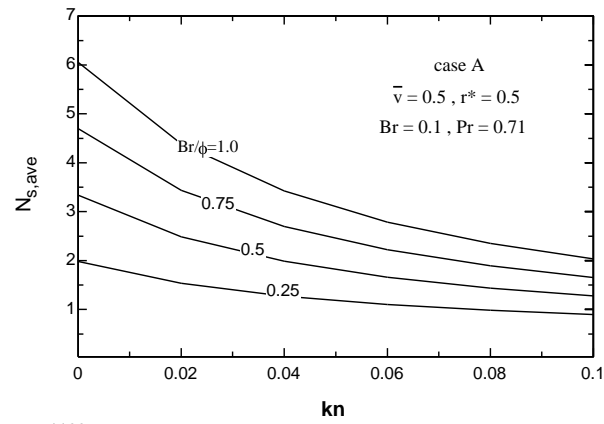


Fig. 4 The variation of  $N_{s,ave}$  for different values of  $Kn, Br/\Omega, r^*$  and  $\bar{v}$  : (a) Case A and (b) Case B





REFERENCES

- [1] A. F. Khadrawi and Ahmad Al-Shyab, "Slip flow and heat transfer in axially moving micro-concentric cylinders," International Communications in Heat and Mass Transfer, 2010.
- [2] W. Marques Jr, G. M. Kremer and F. M. Sharipov, "Couette flow with slip and jump boundary conditions," Continuum Mech. Thermodynamic, vol. 12, pp. 379-386, 2000.

- [3] O. Haddad, M. Abuzaid and M. Al-Nimr, "Entropy generation due to laminar incompressible forced convection flow through parallel plates microchannel," *Entropy*, Vol. 6, No.5, pp. 413-426, 2004.
- [4] O. Aydin and M. Avci, "Heat and fluid flow characteristics of gases in micropipes," *International Journal of Heat and Mass Transfer*, vol. 49, pp.1723-1730, 2006.
- [5] O. Aydin and M. Avci, "Viscous-dissipation effects on the heat transfer in a Poiseuille flow," *Applied Energy*, vol. 83, pp. 495-512, 2006.
- [6] O. Aydin and M. Avci, "Analysis of laminar heat transfer in micro-poiseuille flow," *International Journal of Thermal Sciences*, vol. 46, pp. 30-37, 2007.
- [7] K. Hooman, "Entropy generation for microscale forced convection: effects of different thermal boundary conditions, velocity slip, temperature jump, viscous dissipation, and duct geometry," *International Communications in Heat and Mass Transfer*, vol. 34, pp. 945-957, 2007.
- [8] M. Barkhordari and S. G. Etamad, "Numerical study of slip flow heat transfer of non-Newtonian fluids in circular microchannels," *International Journal of Heat and Fluid Flow*, vol. 28, pp. 1027-1033, 2007.
- [9] W. Sun, S. Kakac and A. G. Yazicioglu, "A numerical study of single-phase convective heat transfer in microtubes for slip flow," *International Journal of Thermal Sciences*, vol. 46, pp.1054-1094, 2007.
- [10] O. Aydin and M. Avci, "Laminar forced convection with viscous dissipation in a Couette-Poiseuille flow between parallel plates," *Applied Energy*, vol. 83, pp.856-867, 2006b.
- [11] M. Avci and O. Aydin, "Laminar forced convection slip-flow in a micro-annulus between two concentric cylinders," *International Journal of Heat and Mass Transfer*, vol. 51, pp. 3460-3467, 2008.
- [12] K. Hooman, "A superposition approach to study slip-flow forced convection in straight microchannels of uniform but arbitrary cross-section," *International Journal of Heat and Mass Transfer*, vol. 51, pp. 3753-3762, 2008.
- [13] M. Yari, "Entropy generation analysis for Couette-Poiseuille flow through parallel-plates microchannel," *International Journal of Exergy*, vol. 6(6), pp. 809-825, 2009.
- [14] M. Yari, "Second-law analysis of flow and heat transfer inside a micro annulus," *International Communications in Heat and Mass Transfer*, vol. 36, pp. 78-87, 2009.
- [15] A. F. Khadrawi and Ahmad Al-Shyyab, "Slip flow and heat transfer in axially moving micro-concentric cylinders," *International Communications in Heat and Mass Transfer*, 2010.
- [16] W. Kays, M. Grawford and B. Weigand, "Convection Heat and Mass Transfer," Mc Graw-Hill, NY, USA, 2005.
- [17] A. Bejan, "Convection Heat Transfer," John Wiley and Sons ed., NY, USA, 2004.
- [18] S. Mahmud, "The second law analysis in fundamental convective heat transfer problems," *International Journal of Thermal Sciences*, vol. 42, pp. 177-186, 2003.
- [19] A. Bejan, "Entropy Generation Minimization," CRC Press, Boca Raton, NY, 1996.

**Sanaz Mirzaparikhany** burned in iran, Ardabil, meshkinshahr in 1985. She is obtained her Bachelor's Degree in Mechanical Engineering in 2008 and Master's degree in 2010 from University of Mohaghegh Ardabili, Iran.

She is TEACHES in the University of Mohaghegh Ardabili and work in field of design and surveying air conditioning, heating, ventilation and refrigeration for house projects. Her main area of research is thermodynamics. She has published 1 research paper in international Journal of Exergy.

**Mehran AbdolalipourAdl** burned in Iran, Ardabil, ardebil in 1987. He is obtained his Bachelor's Degree in Mechanical Engineering in 2010 and Master's degree in 2013 from University of Tabriz, Iran.

**Mortaza Yari** obtained his Bachelor's Degree in Mechanical Engineering in 1992 from Iran University of Science and Technology, Iran, his Master's Degree in 1995 from Tarbiat Modarres University, Iran and PhD in Mechanical Engineering from University of Tabriz, Iran in 2006. He is presently Associate Professor in the University of Mohaghegh Ardabili. His main areas of research are advanced power plant system design and simulation, thermodynamics, air-conditioning, refrigeration and heat pumps systems. He has published over 70 research papers in refereed international journals and conference proceedings. He has also 15 years teaching experience.